Conservation Laws and Gluing Constructions for Constant Mean Curvature (Hyper)Surfaces

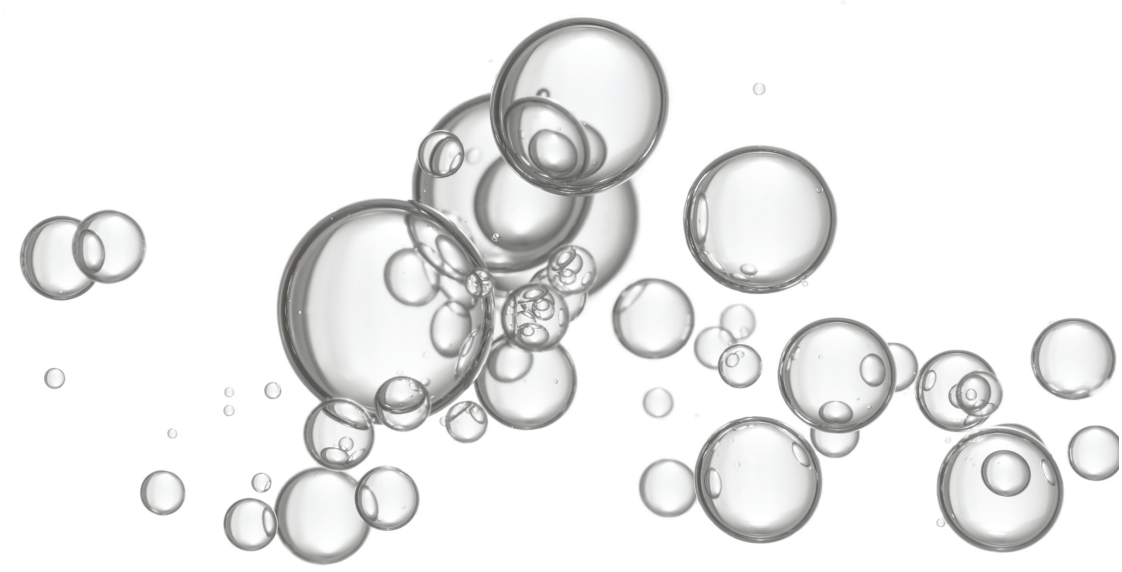

Christine Breiner, Nikolaos Kapouleas, and Stephen Kleene

Christine Breiner is an associate professor of mathematics at Brown University. Her email address is christine_breiner@brown.edu.

Nikolaos Kapouleas is a professor of mathematics at Brown University. His email address is nicolaos_kapouleas@brown.edu.

Stephen Kleene is an assistant professor of mathematics at University of Rochester. His email address is skleene@ur.rochester.edu.

Communicated by Notices *Associate Editor Chikako Mese.*

DOI: https://doi.org/10.1090/noti2473

1. Introduction

In this article, we survey the current status of the theory of constant mean curvature (CMC) hypersurfaces in Euclidean spaces. We give prominence to gluing constructions and conservation laws, and highlight the role of conserved quantities in gluing.

The theory of CMC and minimal surfaces has classical roots in the calculus of variations, a branch of mathematics first investigated by Euler, Lagrange, and others in the 1700's. Among all immersions of surfaces in a Euclidean

space, the complete CMC or minimal immersions can be considered the most interesting on geometric grounds because they are characterized by the constancy of the mean curvature, which is a simple natural geometric condition. CMC surfaces can be characterized as those surfaces for which the area is stationary under compactly supported volume preserving variations, and in physical contexts they arise as interfaces between fluids in stasis in the presence of a pressure jump and surface tension.

1.1. **The mean curvature of hypersurfaces.** The *mean curvature* H of a smooth two-sided hypersurface Σ in a manifold M at a point $p \in \Sigma$ is the average curvature of normal sections through p (once a normal direction is chosen). Equivalently, up to a constant depending only on the dimension, it can be computed as the divergence of the unit normal field ν. That is,

$$H := -\frac{1}{n}\operatorname{Div}_\Sigma(\nu).$$

For hypersurfaces in Euclidean spaces, it is the normal part of the Laplacian of the position vector up to the constant $\frac{1}{n}$:

$$H = \frac{1}{n}\langle \Delta \vec{x}, \nu\rangle.$$

H can be interpreted as the *gradient* of the area functional on surfaces, which we explain below in Section 1.3. It is invariant under isometries of $\mathbb{R}^{n+1}$ and is *homogeneous of degree* -1, meaning that if Σ is dilated by a positive scalar, its mean curvature scales by the reciprocal. A two-sided smooth hypersurface is a *constant mean curvature (CMC)* hypersurface if its mean curvature is a nonzero constant. After possibly exchanging the unit normal for its negative and scaling, we can assume that the mean curvature of a CMC surface is 1. The basic examples of CMC surfaces in Euclidean space are spheres and cylinders. Observe that the constant $\frac{1}{n}$ in the definition of the mean curvature ensures that hyperspheres of radius 1 oriented by the inward pointing normal have mean curvature 1.

Remark 1.1. Throughout this article, unless otherwise specified, the term *surface* will refer to a smooth, complete, connected, two-sided immersed hypersurface in a Euclidean space. Also, *CMC surface* will refer to a surface with mean curvature $H \equiv 1$.

1.2. **Variations and surface area.** Given a surface $\Sigma^n \subset \mathbb{R}^{n+1}$, a (smooth) *variation* is a smooth one parameter family Σ_t of surfaces defined for small t and such that $\Sigma_0 = \Sigma$. A compactly supported vector field X on $\mathbb{R}^{n+1}$ gives rise to a variation of Σ by considering time slices Σ_t of Σ along the flow of X, and we say that this variation is *induced* by the vector field X. If we let $\operatorname{Area}(\Sigma)$ denote the surface area (n-volume) of Σ, the linear change in surface area of $\Sigma_t \setminus \Sigma$ is given by

$$\delta_X \operatorname{Area}(\Sigma) := \frac{d}{dt}\Big|_{t=0} \operatorname{Area}(\Sigma_t \setminus \Sigma) = \int_\Sigma \operatorname{Div}_\Sigma(X).$$

1.3. **The mean curvature as the gradient of area.** Separating the tangential and normal parts, X^T and $X^\perp$, of X and writing $X^\perp = u\,\nu$ gives

$$\operatorname{Div}_\Sigma(X) = \operatorname{Div}_\Sigma(X^T + X^\perp) = \operatorname{Div}_\Sigma(X^T) - nuH.$$

Since X is compactly supported, the first term integrates away by the divergence theorem and we are left with

$$\delta_X \operatorname{Area}(\Sigma) = -n\int_\Sigma uH. \tag{1}$$

Observe that (1) allows us to interpret the mean curvature, up to a constant n, as the negative gradient of the area (where the positive gradient of the area gives the path of steepest ascent): Among L^2 normalized smooth functions u, the choice $u = H$ minimizes $\delta_X \operatorname{Area}(\Sigma)$.

1.4. **Variational characterization of *CMC* surfaces.** A variation of Σ induced by a compactly supported vector field X is *volume preserving* if the (oriented) volume of the region U_t bounded by Σ and Σ_t is stationary at $t = 0$. Here, *oriented* means that the volumes of components of U_t where Σ_t is "above" Σ count positively and those where Σ_t is "below" count negatively. Note that for immersed Σ, some regions of U_t may appear with multiplicity and must be counted appropriately. Alternatively, by appealing to linearity, we could restrict our attention to perturbations supported on embedded parts of Σ.

The linear change in the volume of U_t along the flow is then given by

$$\frac{d}{dt}\Big|_{t=0} \operatorname{Vol}(U_t) = \int_U \operatorname{Div}(X) = \int_\Sigma \langle X, \nu\rangle = \int_\Sigma u.$$

Combining with (1) we see that Σ is stationary under volume preserving variations if and only if, for all smooth compactly supported functions u on Σ,

$$\int_\Sigma u = 0 \implies \int_\Sigma Hu = 0.$$

A basic argument using cutoff functions implies that H is constant.

1.5. **Physical interpretation of mean curvature.** CMC surfaces arise in physical contexts as soap films or as interfaces between fluids in equilibrium. Cohesive forces between molecules on the fluid interface result in surface (or interfacial) tension. If the surface tension coefficient is constant and equal to γ, then the force exerted on the center of an infinitesimal ball R in the soap film by a point on the boundary is approximately the product $\gamma\,\eta$, where η denotes the outward conormal along the boundary. The

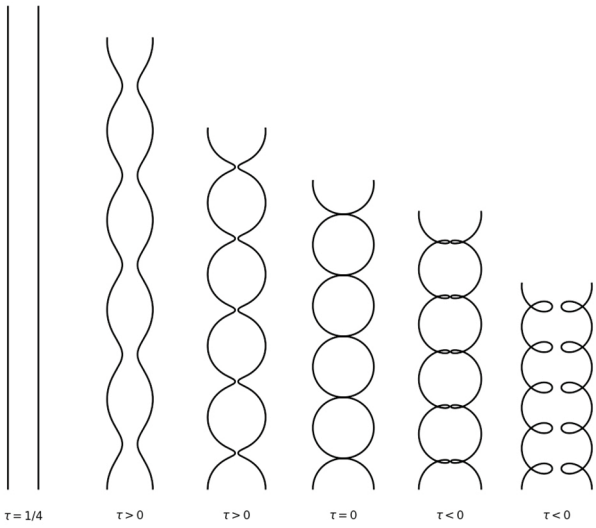

Figure 1. Generating curves for Delaunay surfaces for six values of the parameter τ. The singular model of antipodal spheres occurs when $\tau = 0$.

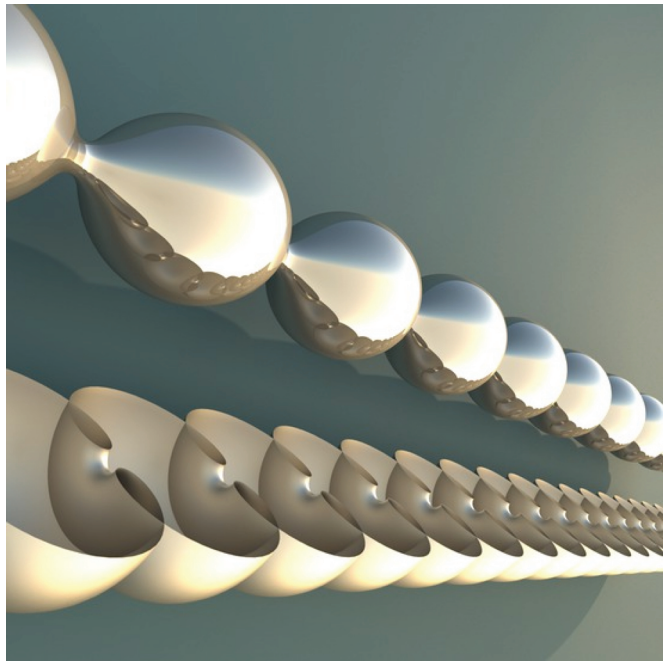

Figure 2. An unduloid and a cutaway of a nodoid.

total force exerted on the center is then approximately the integral

$$\vec{F} \approx \gamma \int_{\partial R} \eta = \gamma \int_R \Delta_\Sigma \vec{x} \approx \gamma H \nu \, dA,$$

where dA denotes the surface area of the infinitesimal ball R and ν the unit normal. Molecules on either side exert a pressure normal to the soap film, and the system is at equilibrium when the jump $\vec{P}$ in pressure across the soap film balances $\vec{F}$, so $\vec{P}+\vec{F} = 0$. Since the system is at equilibrium, the pressure jump is constant strength, so that $\vec{P} = p\nu \, dA$ for some constant p. The equilibrium condition can then be written as $(\gamma H + p)\,\nu = 0$, which is equivalent to the condition that H is constant.

2. History and Examples

2.1. **Classical results.** Although many examples of complete *minimal surfaces* in $\mathbb{R}^3$ were constructed early on using the relation with the theory of one complex variable (Enneper-Riemann-Weierstrass representation), the only early examples of complete *CMC surfaces* of finite topological type were the round sphere, the cylinder and the Delaunay surfaces [Del41]. Discovered in 1841, the Delaunay surfaces form a one-parameter continuous family of rotationally invariant CMC cylinders, which are periodic with translational period along their rotational axis.

We call the parameter τ and it is defined so that when $\tau > 0$ the surfaces are embedded (and called *unduloids*) and when $\tau < 0$ they are not embedded (and called *nodoids*). The explicit value for τ is determined in (10). The unduloids interpolate between a necklace of round spheres (corresponding to $\tau = 0$) and a cylinder (corresponding to $\tau = \frac{1}{4}$). Classically a generating curve for the unduloids can be obtained by tracing the focus of a rolling ellipse. Figure 1 displays generating curves for various values of τ. Each fundamental domain under the translational period is an annulus and consists of both an annulus with Gauss curvature $K > 0$ and a "neck" (an annulus with $K < 0$). See Figure 2 for three-dimensional renderings of two Delaunay surfaces.

As $\tau \to 0$, each annulus with $K > 0$ tends to a sphere in the necklace with two antipodal points removed (where the sphere touches the adjacent spheres). Each neck shrinks to a point (where sphere touching occurs), but if blown up so the waist has unit size, it converges to a catenoid. The limiting behavior prompts us to call compact, connected regions where $K > 0$ *spherical regions* and compact, connected regions where $K < 0$ *catenoidal regions*.

The closed CMC examples are particularly important because there are no closed minimal immersions in the Euclidean spaces by the maximum principle. In 1853, Jellet proved that star-shaped CMC surfaces are round spheres. A century later Hopf established the same for topological CMC spheres [Hop83], and shortly afterwards Alexandrov did the same for embedded CMC surfaces [Ale62]. These results and their methods of proof had a profound influence in mathematics: Hopf introduced the *Hopf differential* which is the (2,0) part of the complexified second fundamental form and is a quadratic holomorphic differential by the Codazzi equation, and Alexandrov introduced the method of reflecting through moving planes which is

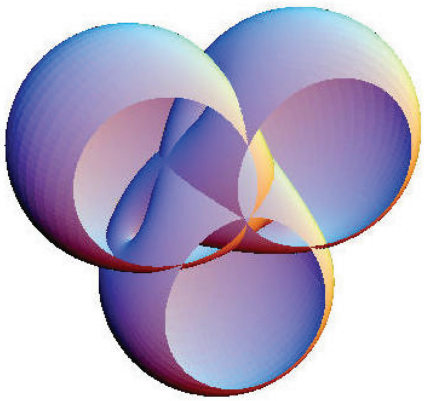

Figure 3. A cutaway of a Wente torus.

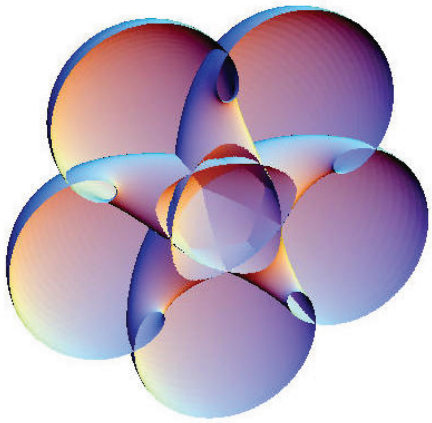

Figure 4. A cutaway of a Wente torus with five spherical regions.

based on the maximum principle. They also motivated the celebrated conjecture (or question according to some) by Hopf on whether the only immersed closed CMC surfaces in Euclidean three-space are round spheres.

2.2. **The Wente tori.** In 1982 Hsiang demonstrated that Hopf's conjecture fails, at least in higher dimensions, by constructing new CMC hyperspheres which are rotationally invariant by a product group and are controlled by an ODE [Hsi82]. Soon afterwards, in a surprising development, Wente carried out a construction of new closed CMC surfaces in $\mathbb{R}^3$ [Wen86]. The Wente examples are tori and his construction was based on the following reduction of the CMC equation to the sinh-Gordon equation on the complex plane $\mathbb{C}$, with z the standard coordinate. $\mathbb{C}$ conformally covers a CMC torus with the Hopf differential taking the form dz^2 over $\mathbb{C}$. If we write the conformal factor as $e^{2w}/4$, the function w on $\mathbb{C}$ is doubly periodic, and by the Gauss equation it satisfies the sinh-Gordon equation

$$\Delta w + \frac{1}{2}\sinh 2w = 0.$$

Conversely given such a w one can integrate to obtain a CMC immersion of the complex plane which is doubly periodic by Euclidean motions. One obtains a CMC torus when the periods close (see Figures 3, 4).

Wente constructed a two-parameter family of such solutions w which integrate to CMC immersions with one translational period and one rotational period. The parameters are the lengths of the sides of a rectangle on which w satisfies a Dirichlet problem and $w > 0$ (and hence $K = 2e^{-2w}\sinh 2w > 0$ also) in the interior. He then extended w to all of $\mathbb{C}$ by odd reflections. The translational period can be closed, reducing the family to a one-parameter family of "Wente cylinders," which are periodic by a rotational period. The rotational period varies continuously in terms of the parameter, and when the rotation is by a rational multiple of π, one obtains a CMC torus. Note that the Wente cylinders have some similarities with the Delaunay cylinders: calling the parameter τ again (see Remark 3.5), the fundamental domain is again an annulus which is the union of one region with $K > 0$ and a region with $K < 0$. (In this case both regions are topological disks.) Moreover as $\tau \to 0$, the region with $K > 0$ tends to a sphere, but now with one point removed, and the region with $K < 0$ again shrinks to a point. The latter region, when blown-up to fixed size, now tends to an Enneper minimal surface.

It is interesting that Wente constructed the solutions w using advanced PDE methods. It was later observed that they could also be constructed by separating variables and solving ODEs in closed form. Further work allowed a classification of all CMC tori by integrable systems methods, including the construction of continuous families of CMC tori. It would be interesting to understand the geometry of these new examples in detail. For example, compelling questions are which minimal surfaces can be obtained as blow-up limits and whether the continuous families of CMC tori can be used in gluing constructions of continuous families of higher-genus closed CMC surfaces.

2.3. **Complete non-compact constructions and characterizations.** In 1988 NK in his thesis carried out a general construction of complete CMC surfaces in $\mathbb{R}^3$ by PDE gluing methods, providing a great variety of examples of any genus with any number of at least two ends, with the only exception being a two-ended torus [Kap90]. Historically, PDE gluing methods had been applied extensively and with great success in Gauge Theories by Donaldson, Taubes, and others. The methods in [Kap90] are more closely related to Schoen's construction of constant scalar curvature metrics in [Sch88]. The theorem is "general" in that no symmetry is required, and it provides a plethora of CMC surfaces. More precisely, given any graph in $\mathbb{R}^3$ satisfying certain conditions outlined below, and for each small enough $\tau \in \mathbb{R}\backslash\{0\}$, a CMC surface can be constructed

as a small perturbation of an *initial surface* explicitly built as described below.

The graphs considered consist of *vertices* which are points in $\mathbb{R}^3$, *edges* which are straight line segments with vertices as endpoints, *rays* which are half-lines with a vertex as an endpoint, and with each edge or ray e assigned a nonzero real number τ_e. Given such a graph, we assign to each vertex p a "force"

$$\vec{F}_p := \sum_e \tau_e \vec{v}_e \in \mathbb{R}^3, \tag{2}$$

where the sum is taken over all the edges and rays with p as an endpoint and $\vec{v}_e$ is the unit vector along e pointing away from p. The given graph in the theorem [Kap90] is a *central graph* whose edges have even integer length and which also has the following properties:

(i) *Balancing*: For each vertex p we have $\vec{F}_p = 0$.
(ii) *Unbalancing*: The graph can be slightly perturbed so that each $\vec{F}_p$ can take any prescribed small value in $\mathbb{R}^3$.
(iii) *Flexibility*: The graph can be slightly perturbed so that each edge length can change by any prescribed small real number.

Families of approximately CMC initial surfaces are then constructed by attaching suitably perturbed Delaunay pieces to unit spheres centered at the vertices (which we will call *vertex spheres*). Each Delaunay piece corresponds to an edge or ray e, has parameter $\tau\tau_e$, and is attached to the vertex sphere(s) centered at its endpoint(s). Finally using the Schauder Fixed Point Theorem it is proved that one of the initial surfaces can be perturbed to exactly CMC. Note that the construction implies that the perturbed Delaunay ends of the CMC surfaces constructed decay exponentially fast to precise Delaunay ends.

The construction of central graphs is easy by elementary means. Note that when $\tau > 0$ and all $\tau_e > 0$, the complete CMC surfaces constructed are *Alexandrov embedded*; that is there is an immersion of a three-manifold Ω into $\mathbb{R}^3$ such that the image of $\partial\Omega$ is the CMC surface. Of these Alexandrov embedded examples only a few very symmetric ones are proved in [Kap90] to be embedded because the construction allows some perturbations which destroy embeddedness.

Around that time, Meeks [Mee88] proved that properly embedded, complete, non-closed CMC surfaces of finite topology have at least two ends each of which is cylindrically bounded. Motivated by this and [Kap90], Korevaar-Kusner-Solomon proved that the Delaunay unduloids are the only properly embedded complete CMC surfaces with finite genus and two ends, and that all Alexandrov properly embedded, complete, non-closed CMC surfaces of finite topology with more than two ends decay exponentially to precise Delaunay ends [KKS89]. Korevaar-Kusner, in [KK93], strengthened these results and made partial progress towards proving the conjecture that all properly embedded finite topology CMC surfaces in $\mathbb{R}^3$ can be associated to a graph in the spirit of the main theorem in [Kap90] discussed above.

Complete CMC surfaces of genus g and $k \geq 3$ ends then attracted much attention. Kusner-Mazzeo-Pollack [KMP96] studied the moduli space of Alexandrov embedded surfaces, $\mathcal{M}_{g,k}$, and proved that it is a real-analytic variety. In particular, every *nondegenerate* (see Section 4.4) $\Sigma \in \mathcal{M}_{g,k}$ is regular in its moduli space, and any perturbation through CMC surfaces near a non-compact, nondegenerate CMC surface must change the asymptotics at infinity. Many aspects of this work are closely tied to, and paved the way for, gluing constructions for nondegenerate objects. We therefore defer a longer discussion of their work to Section 4.4.

Große-Brauckmann [GB93] used a conjugate surface construction to produce surfaces in $\mathcal{M}_{0,k}$ with maximal (k-fold dihedral) symmetry, including those with large neck size. Große-Brauckmann-Kusner-Sullivan and Große-Brauckmann-Korevaar-Kusner-Ratzkin-Sullivan [GBKK$^+$09] determined further results for a subset of the moduli space of $\mathcal{M}_{0,k}$, namely the set of *coplanar k-noids*. (A coplanar k-noid has a plane of symmetry containing all of the asymptotic axes of its ends.) Moreover they show that all coplanar k-noids are nondegenerate. Mazzeo-Pacard, with a gluing construction, produced maximally symmetric CMC surfaces by attaching Delaunay ends to the ends of a nondegenerate Alexandrov embedded minimal surface with finite total curvature, genus g, and k catenoidal ends [MP01]. Mazzeo-Pacard-Pollack carried out a gluing connected sum construction [MPP01] and Ratzkin, in his thesis, an end-to-end gluing construction. Jleli [Jle09] demonstrated the Ratzkin technique can be extended to higher dimensions.

2.4. Closed examples for genus ≥ 2.

Returning now to Hopf's question, note that Wente's construction left it open for genus $g \geq 2$. The general theorem in [Kap90] produced only non-compact complete examples, because although it is possible to find graphs without rays satisfying the balancing and unbalancing conditions, those do not satisfy the flexibility condition since the lengths of some of the edges determine the lengths of the rest. It turned out that it was possible to remedy this difficulty, and in [Kap91] NK constructed closed CMC surfaces of any genus $g \geq 3$. The idea was to vary τ so that the periods of the Delaunay surfaces vary and use very long Delaunay pieces to magnify the effect. This way for some value of τ the Delaunay pieces corresponding to edges whose length cannot be perturbed freely are arranged to "fit."

Even after the construction in [Kap91] the case of genus $g = 2$ remained open because no balanced graphs providing this topology exist. Using Wente tori as building blocks

instead of Delaunay surfaces was a possible approach to overcoming this difficulty. Recall that a Wente torus T with small τ has regions with $K > 0$ each of which approximates a unit sphere with one point removed. Let T_{sph} be such a region. The rest of the torus $T_{rest} := T \setminus T_{sph}$ can then be considered attached to an (approximate) punctured unit sphere. An approximately CMC initial surface of genus g can then be constructed by puncturing a unit sphere at g points, and attaching a copy of T_{rest} at each point. We emphasize that these attachments are not through small necks, as this would contradict balancing as we will describe in Remark 3.4. Instead the attachments imitate the way T_{rest} is attached to T_{sph} in the Wente torus itself.

In [Kap95] NK proved that closed CMC surfaces of any genus $g \geq 2$ can be constructed by correcting such initial surfaces. This required a much deeper understanding of the phenomena involved and a new methodology. It also led to what was called the *geometric principle*, which we describe in Section 4. Together with the new methodology, the geometric principle has now proved instrumental in successfully carrying out many PDE gluing constructions for various geometric objects.

We also mention that Jleli and Pacard produced closed surfaces with high symmetry using an end to end construction and later Jleli extended these ideas to higher dimensions. Jleli's result would provide new symmetric closed examples if a crucial intermediate step, namely the construction of k-ended nondegenerate CMC hypersurfaces, is carried out.

2.5. **Complete non-compact hypersurfaces.** More recently two of the authors [BK14] reworked the construction in [Kap90] following the new approach of [Kap95] to obtain more precise control of the surfaces constructed, proving this way that many more embedded examples exist. Furthermore, overcoming new serious difficulties, they generalized the constructions of [Kap90, BK14] to any higher dimension [BK21]: given a graph in $\mathbb{R}^{n+1}$ and $\tau \neq 0$ as in the $\mathbb{R}^3$ case above, approximately CMC initial surfaces are constructed using n-spheres and pieces of the n-dimensional Delaunay surfaces. (The n-dimensional Delaunay surfaces are $O(n)$-invariant periodic, controlled by an ODE similar to the classical one.) As in the $\mathbb{R}^3$ case, one of these initial surfaces is then perturbed to exactly CMC. We hope that this result will encourage new results in the higher dimensional setting, clarifying this way similarities and differences with the results in $\mathbb{R}^3$.

3. Conservation Laws and Balancing

Every CMC surface satisfies certain conservation laws which arise from an idea clearly articulated by Noether in 1918. While many conserved quantities in physics were previously known, in that work, she established the deep connection between conserved quantities and symmetries of a system. Indeed, she expressed the general principle that if a variational problem is invariant under the action of a continuous group of symmetries, then the variational solutions will satisfy a system of conservation laws. In our current context, this implies that every CMC surface will satisfy conservation laws induced by the isometries of the ambient space. These laws were explicitly determined for CMC surfaces in Euclidean space in [KKS89] and are an important tool in gluing constructions and the classification of CMC surfaces. For an overview of the role of conservation in classification results, the interested reader can consult [BK18].

We outline here the role of conserved quantities for CMC surfaces in manifolds, giving special attention to the Euclidean setting. Given a surface $\Sigma^n \subset \mathbb{R}^{n+1}$, the curvature of Σ is invariant under translations and rotations. Therefore, the CMC variational problem is invariant under these isometries on $\mathbb{R}^{n+1}$ and we expect to find balancing formulas associated with each of these isometries (see (7), (8)).

For the general discussion, we begin with a Riemannian manifold M^{n+1} with metric g and Levi-Civita connection ∇. Given a smooth vector field X on M, we let $\Phi^X : \mathbb{R} \times M \to M$ denote the *flow induced by* X where

$$\Phi^X(t, m) := \gamma_m(t)$$

for the geodesic γ_m satisfying $\gamma_m(0) = m$ and $\dot{\gamma}_m(t) = X(\gamma_m(t))$.

We let $\mathcal{I}(M)$ denote the group of isometries of M–homeomorphisms from M to itself which preserve the metric g. $\mathcal{I}(M)$ is a Lie group which acts smoothly on M. Let $\mathcal{X}(M)$ denote the Lie algebra of smooth vector fields on M with Lie bracket $[X, Y] = XY - YX$. Let $L_X g$ denote the *Lie derivative of g with respect to X*, defined so that for $Y, Z \in \mathcal{X}(M)$,

$$L_X g(Y, Z) = \langle \nabla_Y X, Z \rangle_g + \langle \nabla_Z X, Y \rangle_g.$$

Since one can also interpret the Lie derivative on the $(0,2)$-tensor g by considering

$$L_X g = \frac{d}{dt}\Big|_{t=0} \left((\Phi_t^X)^* g \right),$$

we see that Φ^X flows through isometries of M iff $L_X g = 0$. The sub-algebra of $\mathcal{X}(M)$ satisfying this property is called the space of *Killing fields* on M.

Following the principle previously discussed, we expect that variations of CMC surfaces induced by Killing fields should give rise to conserved quantities. To that end, let $Y \in \mathcal{X}(M)$ be a Killing vector field. Let $\Sigma^n \subset M$ be a smooth embedded surface and let $\Omega^n \subset \Sigma$ be smooth, bounded, open subset with $\partial\Omega = \Gamma$ a smooth $(n-1)$-dimensional submanifold. Let $K^n \subset M$ be smooth and $U^{n+1} \subset M$ be open with $\partial K = \Gamma$ and $\partial U = K \cup \Omega$. Since

Y is Killing, the volumes of Ω, U are preserved under the variation induced by Y. That is,

$$\left.\frac{d}{dt}\right|_{t=0} \mathrm{Area}(\Phi^Y(t,\Omega)) = 0,$$
$$\left.\frac{d}{dt}\right|_{t=0} \mathrm{Vol}(\Phi^Y(t,U)) = 0.$$

By the divergence theorem,

$$0 = \left.\frac{d}{dt}\right|_{t=0} \mathrm{Vol}(\Phi^Y(t,U)) = \int_K \nu_{\mathrm{out}} \cdot Y + \int_\Omega \nu_{\mathrm{out}} \cdot Y \quad (3)$$

where ν_{out} is the outward unit normal to ∂U. Using the divergence theorem again and the definition of mean curvature,

$$0 = \left.\frac{d}{dt}\right|_{t=0} \mathrm{Area}(\Phi^Y(t,\Omega)) = \int_\Gamma \eta \cdot Y - \int_\Omega n H_\Sigma \nu_{\mathrm{in}} \cdot Y \quad (4)$$

where ν_{in} represents the inward pointing normal with respect to Ω.

Note that (3), (4) together imply that

$$n\int_\Omega (H-1)\nu_{\mathrm{in}} \cdot Y = \int_\Gamma \eta \cdot Y - n\int_K \nu_{\mathrm{out}} \cdot Y. \quad (5)$$

We now consider the special case when $H_\Sigma \equiv 1$.

Lemma 3.1. *Let $\Sigma^n \subset M^{n+1}$ be an embedded CMC surface with $H_\Sigma \equiv 1$, $\Gamma \subset \Sigma$ a smooth, null-homologous $(n-1)$-cycle bounding a compact $\Omega \subset \Sigma$, $K \subset M^{n+1}$ a smooth n-cycle with $\partial K = \Gamma$. Let η denote the outward conormal to Σ along Ω and ν_K denote the unit normal on K such that $-\nu_K$ agrees with the orientation on Ω. Then for every Killing field $Y \in \mathcal{X}(M)$,*

$$\int_\Gamma \eta \cdot Y - n\int_K \nu_K \cdot Y = 0. \quad (6)$$

In this article we are of course particularly interested in the consequences of Lemma 3.1 in Euclidean spaces.

Corollary 3.2. *Let $\Sigma^n \subset \mathbb{R}^{n+1}$ be an embedded CMC surface with $H_\Sigma \equiv 1$. Let $\Gamma \subset \Sigma$ be a smooth $(n-1)$-cycle and choose a conormal direction η to Σ along Γ. Let $K \subset \mathbb{R}^{n+1}$ be a smooth n-cycle such that $\partial K = \Gamma$. Let $S \subset \Sigma$ be an open subset of a small neighborhood of Γ such that $\Gamma \subset \partial S$ and η is outward pointing with respect to S. Choose ν_K the unit normal on K such that $-\nu_K$ agrees with the orientation on S. Then*

$$\mathrm{Force}(\Gamma) := \int_\Gamma \eta - n\int_K \nu_K \quad (7)$$

is a homological invariant. Moreover, if $n = 2$, then for $\vec{x}$ the position vector in $\mathbb{R}^3$,

$$\mathrm{Torque}(\Gamma) := \int_\Gamma \eta \times \vec{x} - n\int_K \nu_K \times \vec{x} \quad (8)$$

is also a homological invariant.

Proof. The proofs of (7) and (8) follow easily from (6) once we choose the appropriate vector fields and consider carefully the orientations of η, ν_K.

Let Γ_1, Γ_2 be two $(n-1)$-cycles such that $\Gamma_1 + \Gamma_2$ is null-homologous. Then there exists $\Omega^n \subset \Sigma$ such that $\partial\Omega = \Gamma_1 \cup \Gamma_2$ and (6) applies for appropriately chosen η, K and ν_K. Now suppose that η_1, η_2 are conormals with the same orientation with respect to the homology class of Γ_1, Γ_2. Choosing K_1, K_2 and ν_1, ν_2 as was done in Lemma 3.1, by applying (6) we see that

$$\int_{\Gamma_1} \eta_1 \cdot Y - n\int_{K_1} \nu_{K_1} \cdot Y = \int_{\Gamma_2} \eta_2 \cdot Y - n\int_{K_2} \nu_{K_2} \cdot Y. \quad (9)$$

Now we choose appropriate vector fields. Set $Y_i = \vec{e}_i$, $i = 1, \ldots, n+1$ where $\{\vec{e}_1, \ldots, \vec{e}_{n+1}\}$ is the standard orthonormal basis in $\mathbb{R}^{n+1}$. Substituting each Y_i into (9) and summing over i yields $\mathrm{Force}(\Gamma_1) = \mathrm{Force}(\Gamma_2)$.

If instead we let Y_i correspond to the rotation fields $(x_3, 0, -x_1), (-x_2, x_1, 0), (0, -x_3, x_2)$, (9) takes the form of $\mathrm{Torque}(\Gamma_1) = \mathrm{Torque}(\Gamma_2)$. □

The gluing constructions of [BK14, BK21, Kap90, Kap91] rely on an understanding of the force through a non-trivial cycle on a Delaunay surface so we calculate that here.

Example 3.3. Let Σ be a Delaunay surface with axis parallel to the vector $\vec{v}$. There is only one non-trivial element $[\Gamma] \in H_{n-1}(\Sigma)$ and since the force is a homological invariant to calculate $\mathrm{Force}(\Gamma)$ we can choose Γ to be a waist of Σ, i.e. an $(n-1)$-sphere of smallest cross-sectional radius, $r_{\min}$. Then $\eta \equiv \pm\vec{v}$, where the sign is positive when Σ is embedded and negative when Σ is not embedded.

The attentive reader will note that we have not even defined the force vector for non-embedded surfaces and thus the previous statement should give you pause. Nevertheless, we can make sense of both Lemma 3.1 and Corollary 3.2 on embedded components of a non-embedded Delaunay surface, which will be sufficient for our purposes.

Since we are free to choose any smooth K with $\partial K = \Gamma$, we let K denote the n-disk with $r \in [0, r_{\min}]$ and $\nu_K \equiv \vec{v}$.

With these choices of Γ and K,

$$\begin{aligned}\mathrm{Force}(\Gamma) &= \int_\Gamma \vec{v} - n\int_K \vec{v} \\ &= \left(\pm r_{\min}^{n-1} - r_{\min}^n\right)\omega_{n-1}\vec{v} \\ &:= \tau_\Sigma \omega_{n-1}\vec{v} \end{aligned} \quad (10)$$

where ω_{n-1} is the volume of the standard $(n-1)$-dimensional sphere and τ_Σ is defined via the last equality.

Remark 3.4. Note that (7) and (10) imply that one cannot perform a connected sum construction of closed surfaces (e.g., two Wente tori) by using a small catenoidal bridge (or Delaunay type neck). Indeed, let Σ_1, Σ_2 be two closed CMC surfaces. Connect the two surfaces by a small catenoidal

bridge. By (10), the bridge contains a curve with nonzero force. On the other hand, the curve is null-homologous with respect to each closed surface and thus should have vanishing force after the singular perturbation.

Remark 3.5. Take Γ to be a meridian in the Wente cylinder, for example a topological boundary circle of the annular fundamental domain described earlier which immerses in $\mathbb{R}^3$ as a figure eight. It is possible to calculate that the force through Γ vanishes but the torque is nonzero and determines the parameter τ. This can be compared with the case of Γ in a Delaunay cylinder as in Example 3.3, where the force is nonzero and determines τ, while the torque with respect to a point of the axis vanishes as can be easily demonstrated. This reflects the rotational character of the Wente cylinders.

4. Gluing Constructions

4.1. **General framework.** We begin by providing the general framework for a CMC gluing construction. As we have seen, in the first step of the construction, *building blocks* (that is simpler surfaces which satisfy the geometric condition $H \equiv 1$ exactly) are combined to construct a more complicated initial surface which satisfies the condition approximately. The building blocks and the initial surface depend on a parameter we call τ. We assume that the error $H-1$ on the initial surface, measured in some appropriate weighted $C^{0,\alpha}$ norm $\|.\|_{0,\alpha}$, is arbitrarily small when $|\tau|$ is small enough. Based on this we want to correct the initial surface M to a nearby CMC surface. This CMC surface can be described as a graph of a function f over M (assuming that M is two-sided).

More precisely, let $X : M \to \mathbb{R}^{n+1}$ denote the immersion of the initial surface and ν a global smooth unit normal to X. If $f \in C^2(M)$ is appropriately small, then $X_f := X + f\nu : M \to \mathbb{R}^{n+1}$ is an immersion, and with H and H_f denoting the mean curvature of X and X_f respectively, we have

$$H_f = H + \frac{1}{n}\mathcal{L}f + Q_f,$$

where $\mathcal{L} = \Delta + |A|^2$ is the Jacobi operator, A is the second fundamental form, and Q_f is a quadratic and higher order expression in f and its derivatives with coefficients involving the geometric invariants of X.

We want to find an f satisfying the equation $H_f \equiv 1$. If we ignore the quadratic and higher order terms we seek a function u satisfying the linearized equation

$$\mathcal{L}u = n(1-H). \tag{11}$$

Presuming for a moment that $\mathcal{L}$ is invertible with inverse $\mathcal{L}^{-1}$ and setting $f = u + v$ where $u = n\mathcal{L}^{-1}(1-H)$, the equation $H_f = 1$ reduces to

$$v = -n\mathcal{L}^{-1}Q_{u+v}.$$

Finding a solution v is then equivalent to finding a fixed point for the map

$$v \to -n\mathcal{L}^{-1}Q_{u+v}.$$

It would be reasonable to hope that there is a suitable weighted $C^{2,\alpha}$ norm $\|.\|_{2,\alpha}$, similar to the $\|.\|_{0,\alpha}$ norm above, such that for $E \in C^{0,\alpha}_{loc}(M)$ and $f \in C^{2,\alpha}_{loc}(M)$ we have linear and quadratic estimates

$$\|\mathcal{L}^{-1}E\|_{2,\alpha} \le C\|E\|_{0,\alpha}, \qquad \|Q_f\|_{0,\alpha} \le C\|f\|^2_{2,\alpha},$$

where $C > 0$ is a uniform constant independent of τ. Assuming this to be the case, we expect to find a fixed point for the map above by using the smallness of $\|H-1\|_{0,\alpha}$, and hence of $\|u\|_{2,\alpha}$, and employing some fixed point theorem. In the most interesting geometric cases however this does not happen and therefore we are forced to modify the approach. The necessary modifications relate to deep geometric and analytic insights which illuminate the nature and difficulties of these constructions.

4.2. **First general constructions** [Kap90]. We concentrate now on the construction in [Kap90]. It is worth mentioning two instructive examples where the construction has to fail. First, consider a "dumbell" construction where the initial surface consists of two unit spheres joined by a catenoidal bridge (or Delaunay type neck). The support of $H-1$ is on two annuli on the spherical regions (slightly perturbed). However, this initial surface cannot be corrected to be CMC because this would contradict both Alexandrov's and Hopf's theorems; it would also contradict the "no connected sum by catenoidal bridges" argument (see Remark 3.4). This is consistent with the theorem in [Kap90] since the corresponding graph consists of a single edge and two vertices and so cannot satisfy the balancing condition $\vec{F}_p = 0$.

Even more striking is the second example where we attempt to construct an embedded torus by bending an unduloid. We introduce a slight bending on each spherical region creating an angle θ between the axes of subsequent necks; the surface becomes a torus with a very large number of spherical regions for suitable discrete values of θ. In this case $H-1$ is supported on spherical regions again, but with $\|H-1\|_{0,\alpha} \sim \theta$ independently of the parameter τ of the unduloid. However small θ is chosen, the construction cannot work because it would contradict Alexandrov's theorem. Note also that the bending, however small, violates balancing.

The question therefore arises: at which step does the general framework outlined above fail and how is this remedied?

Note that on the initial surfaces in [Kap90] (whose construction was outlined in Section 2.3), $H-1$ is supported on annuli on the spherical regions where the attachment of the Delaunay pieces occurs. The geometry there is close

to that of the unit sphere and each attachment annulus is rotationally invariant around the axis of the piece being attached. It is easy to calculate that $\|H-1\|_{0,\alpha} \sim |\tau|$ and so far there are no difficulties.

The framework fails when we need the linear estimate. This is due to the existence of small eigenvalues for $\mathcal{L}$. Indeed as $\tau \to 0$ each spherical region tends to a unit sphere where the linearized operator has a three-dimensional kernel consisting of the first harmonics. One approach to resolving this difficulty is to understand the small eigenvalues on the initial surface globally and proceeding accordingly.

NK introduced a simpler approach in [Kap90]: one solves the linearized equation modulo the *substitute kernel*, a space $\mathcal{K} \subset C^\infty(M)$. $\mathcal{K}$ is spanned by a collection of functions, each supported on a single spherical region and "substituting" for one first harmonic on that spherical region. (For completeness of the exposition we mention that in [Kap90] "spherical regions" includes the catenoidal bridges; for details we refer to the original paper). One can then solve semi-locally modulo $\mathcal{K}$ and combine the ensuing solutions to get a global one by using the decay of the semi-local solutions. The decay is established by comparing to the limit as $\tau \to 0$; recall that in the limit, adjacent spherical regions disconnect.

Solving the linear equation modulo $\mathcal{K}$ only postpones the difficulty since in the end we will get $H_f - 1 \in \mathcal{K}$ instead of $H_f - 1 = 0$ as desired. This is where balancing and unbalancing are used. By (5) the L^2 inner product of $H_f - 1$ (or $H-1$) with the components of the unit normal equals the sum of boundary terms. Each boundary term can be calculated as in (10) (with $\vec{v}$ replaced by $\vec{v}_e$ and τ_Σ replaced by $\tau\tau_e$). Observe that on the vertex spheres, the sum of these terms can be approximated by the $\vec{F}_p$'s defined in (2) (up to a constant). The balancing condition then implies that the $\mathcal{K}$ content is small, and the unbalancing condition implies that we can approximately prescribe it. We can therefore make $H_f - 1$ vanish exactly by choosing the correct values for the unbalancing parameters via the fixed point theorem.

4.3. **Gluing Wente tori** [Kap95]. We proceed now to discuss the construction in [Kap95] which contains new ideas which have been the basis for many other gluing constructions for various geometric objects. A simple attempt to follow the same approach as in [Kap90] stumbles on two differences between Delaunay and Wente cylinders:

(i) Each spherical region S is attached to the rest of the Wente cylinder at a single point and its boundary ∂S is connected. The force through ∂S in the sense of (7) therefore has to vanish by Lemma 3.1. This is different from the case of a Delaunay cylinder where there are two points of attachment and ∂S has two connected components, each of which has nonzero force. In the Delaunay case by transiting on S to a slightly different Delaunay surface we can unbalance and create $H-1$ along the first harmonics on S. This is clearly not possible in the Wente case.

(ii) In both cases *transition regions* are defined to be (connected) neighborhoods of $\{K = 0\}$. The difference is that in the Delaunay case they are annuli each of which connects two adjacent spherical regions, while in the Wente case there is only one transition region connecting to each spherical region. This makes decay issues much harder to handle.

These problems were resolved using the following ideas.

(a) *The extended substitute kernel.* In [Kap95] NK expanded the idea of the substitute kernel he had introduced in [Kap90] by enlarging the substitute kernel $\mathcal{K}$ to a larger space called the *extended substitute kernel*, $\widetilde{\mathcal{K}}$. Solving the inhomeogeneous equation $\mathcal{L}u' = E$ modulo $\widetilde{\mathcal{K}}$ ensures not only the existence of a solution u' as before, but also that u' satisfies very strong decay estimates along the transitions regions where a power of τ is gained from one spherical region to the next.

(b) *The geometric principle.* As in the case of the substitute kernel, solving the linear equations modulo the extended substitute kernel $\widetilde{\mathcal{K}}$ may lead to satisfying the CMC condition only modulo $\widetilde{\mathcal{K}}$; that is $H_f - 1 \in \widetilde{\mathcal{K}}$. To remedy this we have to introduce parameters in the construction of the initial surfaces which prescribe a component of $H-1$ as any small element of $\widetilde{\mathcal{K}}$ with the rest of $H-1$ considered an error. It turns out that all the elements of $\widetilde{\mathcal{K}}$ can be associated with ambient Killing fields on parts of the initial surface. The geometric principle says that prescribing those elements can be achieved by introducing *dislocations* where some parts of the initial surface are repositioned relative to the rest by flowing them along those ambient Killing fields. Note that in retrospect this is true for example for the unbalancing parameters in [Kap90] because the Delaunay pieces are repositioned relative to the central spherical regions. Since then the geometric principle has played a fundamental role in designing the setup of many gluing constructions for other geometric objects.

(c) *The implementation of the geometric principle.* The implementation of the geometric principle requires understanding and estimating the Dirichlet problem for the linear operator $\mathcal{L}$ on the transition regions. The Dirichlet data is given by the action of the Killing fields corresponding to the dislocations. The approximate rotational invariance of (parts of) the transition region combined with separation of variables plays an important role.

(d) *Ideas particular to Wente tori.* In the case of [Kap95] estimating the solutions and implementing the geometric principle is particularly challenging because of the involved geometry and topology of the transition regions. In order to monitor the creation of the extended substitute kernel, (5) is used with Ω an annulus consisting of a spherical region and its opposing Enneper-like neck. The $\partial\Omega$ consists of two immersed circles each resembling a "figure eight." The Killing field Y can be either translational or rotational; the extended substitute kernel content on Ω is expressed in terms of forces and torques through these "figure eight" circles. The Wente cylinders are conformally flat and these forces and torques can be calculated by using separation of variables and the symmetries involved.

Another interesting feature in the proof is how the period closing, which is relevant as in [Kap91], is related to proving that the final surfaces satisfy $H = 1$. Finally note that there are a number of interesting ideas related to estimating the creation of extended substitute kernel which we do not discuss here.

4.4. **More examples of finite topology.** Other gluing constructions mentioned in Section 2 adopt a different approach than those outlined above. In particular, they work with building blocks which are *nondegenerate*, which greatly simplifies the linear problem. A surface Σ is called *nondegenerate* if the only function $f \in L^2$ satisfying $\mathcal{L}f = 0$ is $f \equiv 0$. By classical PDE results, on every compact subset of a nondegenerate surface Σ, one can easily find a function u satisfying (11) with good estimates.

We define the space of *Jacobi functions* on a surface Σ to be the set of all functions φ satisfying $\mathcal{L}\varphi = 0$ on Σ. The Jacobi functions on a Delaunay unduloid can be determined by exploiting the rotational symmetry to use a Fourier decomposition and solve appropriate ODEs, but the lower mode functions also have a geometric interpretation. For any Killing vector field Y, $\mathcal{L}(Y \cdot \nu) = 0$, and thus every Killing field determines a Jacobi function. In particular, for a Delaunay unduloid $\Sigma^n \subset \mathbb{R}^{n+1}$, the $n+1$-dimensional space of translations and $n(n+1)/2$-dimensional space of rotations orthogonal to the Delaunay axis induce *geometric* Jacobi functions. One additional geometric function is induced by varying the parameter τ. All of the geometric Jacobi functions have sub-exponential growth, while all of the high mode Jacobi functions either grow or decay exponentially. Note that the geometric Jacobi functions also naturally play a crucial role in the gluing constructions outlined in the other subsections.

In [KMP96], the starting point to understanding $\mathcal{M}_{g,k}$ is the asymptotic result in [KKS89]; namely, if $\Sigma \in \mathcal{M}_{g,k}$ then each end of Σ converges exponentially fast to a Delaunay end. Given a nondegenerate surface in $\mathcal{M}_{g,k}$, any perturbation through CMC surfaces necessarily changes the asymptotics. Therefore, surfaces near a nondegenerate Σ cannot have the same asymptotic Delaunay ends as Σ; thus the surfaces cannot be described as normal graphs over Σ but instead as normal graphs over a surface with perturbed ends. These perturbations are given by variations using the geometric Jacobi functions for each asymptotic Delaunay end. Understanding $\mathcal{M}_{g,k}$ then follows from determining the linearized operator is surjective onto a weighted Sobolev space, understanding the decomposition of solutions into the sum of a perturbation function and an exponentially decaying function, and finding the null space of the linear operator.

The gluing constructions of [MP01, MPP01] perform linear analysis similar to that of [KMP96], though they work with weighted Hölder rather than weighted Sobolev spaces. In [MP01], the authors glue Delaunay ends onto an appropriately truncated nondegenerate minimal k-noid (a minimal surface with k catenoidal ends and possibly positive genus). The construction relies on matching Cauchy data across the gluing interfaces–which can be accomplished since Delaunay necks, under rescaling, converge on compact sets to a catenoid. Using similar ideas, [MPP01] determine a more general setup. Given two nondegenerate CMC surfaces with boundary, Σ_1, Σ_2, presume the surfaces are oriented such that the two tangent planes agree at 0 and their normals are oppositely oriented. They construct a family of CMC surfaces with boundary that degenerate to $\Sigma_1 \cup \Sigma_2$ as the parameter of the family tends to zero. The goal here is again to match Cauchy data across gluing interfaces, and in this case the authors use the nondegeneracy to modify the surfaces, at the point of tangency, by a Green's function for their respective linear operators which has a pole at the tangent point. Between these perturbed surfaces they insert a catenoidal neck and they match the data by truncating the surfaces appropriately.

In a later work, Mazzeo-Pacard-Pollack [MPP05] extend the ideas of [MPP01] to the non-compact setting. Starting with a nondegenerate $\Sigma \in \mathcal{M}_{g,k}$, they produce a nondegenerate $\Sigma' \in \mathcal{M}_{g,k+1}$ by gluing in a Delaunay end at any point $p \in \Sigma$. (Actually for each p they construct a one parameter family of such surfaces.) Again they use the nondegeneracy of Σ to modify by a Green's function with pole at the point p. They match Cauchy data between the Green's function and the Delaunay end, which can be done since both, under dilation, converge on compact sets to a catenoid.

4.5. **A general construction in higher dimensions [BK21].** In [BK14, BK21], the authors improve upon the results of [Kap90] to produce new embedded examples of finite topological type and infinitely many new (embedded and immersed) higher dimensional CMC surfaces. In both papers they apply the techniques developed in [Kap95]—

namely the geometric principle and the extended substitute kernel—to a setting without symmetries. Among other things, these allow them to produce linear solutions which decay fast enough to preserve embeddedness in all of the expected initial configurations. The decay is prescribed by varying the family of initial surfaces by dislocations (induced by the flow of Killing fields) between the central spherical regions and the Delaunay pieces attached to them. Given a vertex sphere, each attached Delaunay piece varies independent of all other pieces and an important aspect of this construction is demonstrating that independence.

The construction in [BK21] induced further advancements and new techniques. First, the linear step of the argument is complicated by the fact that the Laplacian is not conformally covariant in high dimensions. In [Kap90, BK14], the linear problem on the catenoidal necks of the Delaunay surfaces is simplified by using a conformal metric which compactifies the surfaces by making them isometric to the spherical regions. In the higher dimensional setting, one must redesign the linear theory. The authors accomplish this by working directly with the induced metric on the catenoidal necks and exploiting the rotational symmetry to use Fourier decompositions on the meridians. A similar complication arises on the transition regions, which are conformal to flat cylinders in two dimensions. For the higher dimensional problem, the authors demonstrate that the linearized operator on the transition regions is sufficiently close to the operator on a flat annulus (in an appropriately weighted metric) to find solutions and determine necessary estimates.

The second major advancement in [BK21] was inspired by the necessary modifications to the linear theory. In [Kap90, BK14], the semi-local solutions on the Delaunay pieces satisfy a Dirichlet condition and therefore can only be expected to solve the linear equation modulo $\mathcal{K}$. In [BK21], the authors exploit the Fourier decomposition. They demonstrate that the linearized operator is invertible for the high modes, while for the low modes they solve a second order ODE with initial data that allows the solutions to grow (slowly) in one direction. As a result, functions of $\mathcal{K}$ are supported only on the vertex spheres rather than on every standard region.

Finally, in [BK21] the authors improve the error estimate for the unbalancing by using a balancing formula on the final hypersurface rather than monitoring the error at each step.

References

[Ale62] A. D. Aleksandrov, *Uniqueness theorems for surfaces in the large. V*, Amer. Math. Soc. Transl. (2) **21** (1962), 412–416. MR0150710

[BK14] Christine Breiner and Nikolaos Kapouleas, *Embedded constant mean curvature surfaces in Euclidean three-space*, Math. Ann. **360** (2014), no. 3-4, 1041–1108, DOI 10.1007/s00208-014-1056-0. MR3273652

[BK21] Christine Breiner and Nikolaos Kapouleas, *Complete constant mean curvature hypersurfaces in Euclidean space of dimension four or higher*, Amer. J. Math. **143** (2021), no. 4, 1161–1259, DOI 10.1353/ajm.2021.0030. MR4291252

[BK18] Christine Breiner and Stephen J. Kleene, *Group actions in the existence and classification of constant mean curvature surfaces*, Handbook of group actions. Vol. III, Adv. Lect. Math. (ALM), vol. 40, Int. Press, Somerville, MA, 2018, pp. 461–484. MR3888626

[Del41] C. Delaunay, *Sur la surface de revolution dont la courbure moyenne est constant*, Journal de Mathématiques Pures et Appliquees **6** (1841), 309–320.

[GB93] Karsten Große-Brauckmann, *New surfaces of constant mean curvature*, Math. Z. **214** (1993), no. 4, 527–565, DOI 10.1007/BF02572424. MR1248112

[GBKK+09] Karsten Große-Brauckmann, Nicholas J. Korevaar, Robert B. Kusner, Jesse Ratzkin, and John M. Sullivan, *Coplanar k-unduloids are nondegenerate*, Int. Math. Res. Not. IMRN **18** (2009), 3391–3416, DOI 10.1093/imrn/rnp058. MR2535004

[Hop83] Heinz Hopf, *Differential geometry in the large*, Lecture Notes in Mathematics, vol. 1000, Springer-Verlag, Berlin, 1983. Notes taken by Peter Lax and John Gray; With a preface by S. S. Chern, DOI 10.1007/978-3-662-21563-0. MR707850

[Hsi82] Wu-yi Hsiang, *Generalized rotational hypersurfaces of constant mean curvature in the Euclidean spaces. I*, J. Differential Geometry **17** (1982), no. 2, 337–356. MR664499

[Jle09] Mohamed Jleli, *End-to-end gluing of constant mean curvature hypersurfaces* (English, with English and French summaries), Ann. Fac. Sci. Toulouse Math. (6) **18** (2009), no. 4, 717–737. MR2590386

[Kap90] Nicolaos Kapouleas, *Complete constant mean curvature surfaces in Euclidean three-space*, Ann. of Math. (2) **131** (1990), no. 2, 239–330, DOI 10.2307/1971494. MR1043269

[Kap91] Nicolaos Kapouleas, *Compact constant mean curvature surfaces in Euclidean three-space*, J. Differential Geom. **33** (1991), no. 3, 683–715. MR1100207

[Kap95] Nikolaos Kapouleas, *Constant mean curvature surfaces constructed by fusing Wente tori*, Invent. Math. **119** (1995), no. 3, 443–518, DOI 10.1007/BF01245190. MR1317648

[KKS89] Nicholas J. Korevaar, Rob Kusner, and Bruce Solomon, *The structure of complete embedded surfaces with constant mean curvature*, J. Differential Geom. **30** (1989), no. 2, 465–503. MR1010168

[KK93] Nick Korevaar and Rob Kusner, *The global structure of constant mean curvature surfaces*, Invent. Math. **114** (1993), no. 2, 311–332, DOI 10.1007/BF01232673. MR1240641

[KMP96] R. Kusner, R. Mazzeo, and D. Pollack, *The moduli space of complete embedded constant mean curvature surfaces*, Geom. Funct. Anal. **6** (1996), no. 1, 120–137, DOI 10.1007/BF02246769. MR1371233

[MP01] Rafe Mazzeo and Frank Pacard, *Constant mean curvature surfaces with Delaunay ends*, Comm. Anal. Geom. **9** (2001), no. 1, 169–237, DOI 10.4310/CAG.2001.v9.n1.a6. MR1807955

[MPP01] Rafe Mazzeo, Frank Pacard, and Daniel Pollack, *Connected sums of constant mean curvature surfaces in Euclidean 3 space*, J. Reine Angew. Math. **536** (2001), 115–165, DOI 10.1515/crll.2001.054. MR1837428

[MPP05] Rafe Mazzeo, Frank Pacard, and Daniel Pollack, *The conformal theory of Alexandrov embedded constant mean curvature surfaces in* $\mathbb{R}^3$, Global theory of minimal surfaces, Clay Math. Proc., vol. 2, Amer. Math. Soc., Providence, RI, 2005, pp. 525–559, DOI 10.1515/crll.2001.054. MR2167275

[Mee88] William H. Meeks III, *The topology and geometry of embedded surfaces of constant mean curvature*, J. Differential Geom. **27** (1988), no. 3, 539–552. MR940118

[Sch88] Richard M. Schoen, *The existence of weak solutions with prescribed singular behavior for a conformally invariant scalar equation*, Comm. Pure Appl. Math. **41** (1988), no. 3, 317–392, DOI 10.1002/cpa.3160410305. MR929283

[Wen86] Henry C. Wente, *Counterexample to a conjecture of H. Hopf*, Pacific J. Math. **121** (1986), no. 1, 193–243. MR815044

Christine Breiner

Nikolaos Kapouleas

Stephen Kleene

Credits

The opening image is courtesy of dkidpix via Getty.

Figure 1 is courtesy of Stephen Kleene.

Figure 2 is courtesy of Dr. Nicholas Schmitt.

Figures 3 and 4 are courtesy of Wayne Rossman. Reprinted by permission from Springer Nature, *Geometriae Dedicata*, "The Morse Index of Wente Tori" by Wayne Rossman, 1969.

Photo of Christine Breiner is courtesy of Nick Dentamaro/Brown University.

Photo of Nikolaos Kapouleas is courtesy of Dimitrios Tzatzos.

Photo of Stephen Kleene is courtesy of Stephen Kleene.